Effect of Transverse Curvature on the Stability of Compressible Boundary Layers

Robert E. Spall* and Mujeeb R. Malik†
High Technology Corporation, Hampton, Virginia 23666

Linear stability theory is used to determine the effect of transverse curvature on the estimated location of the onset of transition for supersonic boundary layers. Results have been obtained for Mach 5 and Mach 1.25 boundary layers formed over cylinders and sharp cones. As transverse curvature increases, the growth rates for the first mode (asymmetric) instability increase, whereas those for the second mode decrease. The overall effect of increasing curvature is to lower the transition Reynolds number at the Mach numbers studied. Transverse curvature is also shown to introduce an apparent unit Reynolds number effect on transition location; for a given cylinder, the transition Reynolds number increases with the increasing unit Reynolds number.

Introduction

In recent years considerable interest has been focused on the development and application of compressible linear stability theory. This has been brought about, in part, by the need to predict laminar/turbulent transition over hypersonic vehicles such as the aerospace plane. Equally important perhaps is the confidence generated by successful correlations at high speeds of experimental transition data with theoretical results based on linear stability theory. For instance, data obtained using conventional supersonic wind tunnels indicated that transition on a cone occurred at a higher Reynolds number than on a flat plate (see Ref. 1). In contrast, e^N calculations based on linear stability theory gave opposite results.[2,3] This discrepancy was resolved when an experiment performed in the NASA Langley Low Disturbance Tunnel vindicated the e^N calculations.[4] Thus, in general, the e^N method provides a practical means for investigating laminar flow-control applications and the estimation of the onset of transition in low-disturbance environments.

The numerical calculations for the compressible stability of flat-plate boundary layers over a wide range of flow conditions were performed by Mack (for a comprehensive review see Ref. 5). Mack obtained a number of important results and demonstrated the existence of higher instability modes. These inviscid modes appear whenever the mean flow relative to the disturbance phase velocity is supersonic. Above about $M=4$, the first of these modes, called the second mode, is most unstable. The prediction by Lees[6] that wall cooling could be used to stabilize the boundary layer was dispelled by Mack. In fact, Mack[7] showed that the second mode instability is actually destabilized by cooling. Demetriades[8] provided experimental verification of Mack's findings regarding the effect of cooling on the second mode.

Stability calculations of a compressible boundary layer over a sharp cone at a zero angle of attack have been performed by Malik,[9] Mack,[2] Gasperas,[10,11] and Malik and Spall.[12] Mack indicates that the inclusion of transverse curvature terms in the computed mean flow has little effect on the planar stability calculations for a 7-deg half-angle cone at Mach 6.8. Malik and Spall[12] provide plots of mean flow temperature and velocity profiles at Mach 5 for 2- and 10-deg cone half-angles, both with and without curvature terms. They found that the effect of neglecting curvature on the mean flow is small for the 10-deg cone but significant for the 2-deg cone. No attempt was made to determine the effect on the stability calculations. They did, however, report that mean flow transverse curvature effects were important when computing the second mode stability characteristics of a series of thin-cylinder boundary layers. The effect of increasing curvature was stabilizing and resulted in an upward shift of the unstable frequency band. Gasperas[10] found a small stabilizing influence when some of the transverse curvature terms were included in the parallel flow stability equations. To date, the effect of transverse curvature terms in the mean flow and stability equations on N-factor calculations has not been reported.

Duck[13] obtained an asymptotic solution for the inviscid axisymmetric stability of a hypersonic boundary layer over a thin cylinder. The radius of the cylinder was restricted to the order of the boundary-layer thickness. His results indicated that curvature effects are stabilizing with respect to both first and second mode axisymmetric disturbances.

Cone stability experiments have been performed by Kendall,[14] Demetriades,[15] and Stetson et al.[16] Major disagreements between these experimental results and the stability calculations still exist. For instance, the experiments all show a range of unstable frequencies above those associated with the second mode disturbances. These unstable bands have not been predicted using linear stability theory.

In the present study, we investigate the effect of transverse curvature on transition location as predicted using the e^N method. For the purposes of this paper, transition location is equated to the location where the disturbance amplitude ratio (A/A_0), as calculated from linear stability theory, first reaches a value of e^9. We consider the boundary layer over a series of adiabatic wall cones and cylinders at Mach 5, and adiabatic wall cylinders at Mach 1.25. The nonsimilar mean flow calculations are performed using a compressible boundary-layer code developed by Harris and Blanchard.[17] For the cylinders, the effect of transverse curvature is included in the calculation of both the mean flow and the stability results. For the sharp cone cases, mean flows are computed both with and without transverse curvature terms. Stability results are computed by including the transverse curvature terms. An apparent unit Reynolds number effect due to the nonsimilar mean flow profiles is also investigated.

Problem Formulation and Numerical Method

The goal of linear stability theory is to determine the response of some predetermined mean flow to an infinitesimally small disturbance. In this study, the mean flow is taken to be

Received March 19, 1990; revision received July 30, 1990; accepted for publication Aug. 1, 1990.

*Research Scientist, 28 Research Drive. Member AIAA.
†President, 28 Research Drive. Senior Member AIAA.

the solution of the compressible boundary-layer equations for a perfect gas. In particular, we consider the "quasiparallel" linear stability of a compressible boundary layer over conical, cylindrical, and flat-plate configurations.

A brief discussion of the boundary-layer equations is in order. The mean flow is given by the solution to the two-dimensional/axisymmetric compressible boundary-layer equations

$$\bar{\rho}\bar{u}\frac{\partial \bar{u}}{\partial x}+\bar{\rho}\bar{v}\frac{\partial \bar{u}}{\partial y}=-\frac{d\bar{p}}{dx}+\frac{1}{r^j}\frac{\partial}{\partial y}\left(r^j\bar{\mu}\frac{\partial \bar{u}}{\partial y}\right) \tag{1}$$

$$\frac{\partial}{\partial x}(r^j\bar{\rho}\bar{u})+\frac{\partial}{\partial y}(r^j\bar{\rho}\bar{v})=0 \tag{2}$$

$$\bar{\rho}\bar{c}_p\bar{u}\frac{\partial \bar{T}}{\partial x}+\bar{\rho}\bar{c}_p\bar{v}\frac{\partial \bar{T}}{\partial y}=\frac{1}{r^j}\frac{\partial}{\partial y}\left(r^j\bar{k}\frac{\partial \bar{T}}{\partial y}\right)+\bar{\mu}\left(\frac{\partial \bar{u}}{\partial y}\right)^2+\bar{u}\frac{d\bar{p}}{dx} \tag{3}$$

where $\bar{u}$ and $\bar{v}$ are the velocity components in the x and y directions, respectively, $\bar{p}$ is the pressure, $\bar{\rho}$ is the density, $\bar{\mu}$ is the first coefficient of viscosity, $\bar{T}$ is the temperature, $\bar{k}$ is the thermal conductivity, and $\bar{c}_p$ is the specific heat. In the foregoing equations, $j=0$ for two-dimensional and $j=1$ for axisymmetric flows. The boundary-layer equations are singular at $x=0$. In order to remove this singularity and provide for a nearly constant boundary-layer thickness in the computational domain, we utilize the Mangler-Levy-Lees[18] transformation

$$d\xi=\rho_e\mu_e u_e r_0^{2j}\,dx \tag{4a}$$

$$d\eta=\left[u_e/\sqrt{(2\xi)}\right]r^j\bar{\rho}\,dy \tag{4b}$$

where the subscript e refers to edge values. We define three new computational variables

$$F=\frac{\bar{u}}{u_e} \tag{5a}$$

$$V=\frac{2\xi}{\rho_e\mu_e u_e r_0^{2j}}\left[F\left(\frac{\partial \eta}{\partial x}\right)+\frac{\bar{\rho}\bar{v}r^j}{\sqrt{2\xi}}\right] \tag{5b}$$

$$\theta=\frac{\bar{T}}{T_e} \tag{5c}$$

and write the boundary-layer equations as

$$\frac{\partial}{\partial \eta}\left(a_1\frac{\partial F}{\partial \eta}\right)-V\frac{\partial F}{\partial \eta}+a_2(\theta-F^2)=2\xi F\frac{\partial F}{\partial \xi} \tag{6}$$

$$\frac{\partial V}{\partial \eta}+F=-2\xi\frac{\partial F}{\partial \xi} \tag{7}$$

$$\frac{\partial}{\partial \eta}\left(a_3\frac{\partial \theta}{\partial \eta}\right)-V\frac{\partial \theta}{\partial \eta}+a_4\left(\frac{\partial F}{\partial \eta}\right)^2=2\xi F\frac{\partial \theta}{\partial \xi} \tag{8}$$

In the aforementioned equations,

$$a_1=(1+\chi)^{2j}\frac{\bar{\rho}\bar{\mu}}{\rho_e\mu_e} \tag{9a}$$

$$a_2=\left(\frac{2\xi}{u_e}\right)\frac{du_e}{d\xi} \tag{9b}$$

$$a_3=\frac{a_1}{\sigma} \tag{9c}$$

$$a_4=(\gamma-1)M_e^2a_1 \tag{9d}$$

Note that $\chi\equiv y/r_0\cos\lambda$ is the "transverse curvature" term, where λ and r_0 are given in Fig. 1. In addition, M is the Mach number and σ the Prandtl number. Transverse curvature is expected to affect the mean flow profiles significantly for cases in which the thickness of the boundary layer is not negligible relative to the body radius r_0. If in the case of a cylinder or sharp cone configuration, the transverse curvature term is neglected, Eqs. (6–8) reduce to a set of similar equations. Then, for identical edge conditions, the cone profiles are thinner than the flat-plate and cylinder profiles by a factor of $\sqrt{3}$ at common streamwise locations.

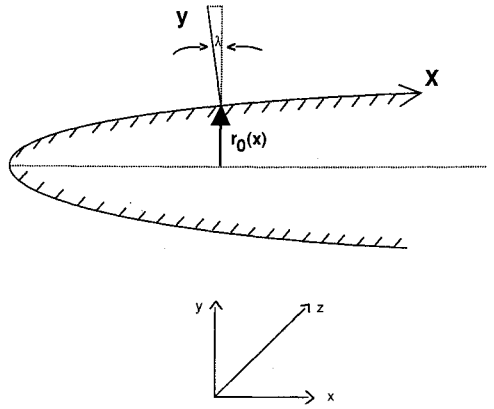

Fig. 1 Coordinate system and notation.

The linear stability equations are derived from the compressible Navier-Stokes equations. The Navier-Stokes equations, nondimensionalized with appropriate constant free-stream reference values and some reference length l, are written as

$$\rho\left[\frac{\partial \boldsymbol{u}}{\partial t}+(\boldsymbol{u}\cdot\nabla)\boldsymbol{u}\right]=-\nabla p+\frac{1}{R}\nabla\cdot\left[\lambda(\nabla\cdot\boldsymbol{u})\bar{I}\right]+\frac{1}{R}\nabla\cdot\left[\mu(\nabla\boldsymbol{u}+\nabla\boldsymbol{u}^{tr})\right] \tag{10}$$

$$\frac{\partial \rho}{\partial t}+\nabla\cdot\rho\boldsymbol{u}=0 \tag{11}$$

$$\rho c_p\left[\frac{\partial T}{\partial t}+(\boldsymbol{u}\cdot\nabla)T\right]-(\gamma-1)M_e^2\left[\frac{\partial p}{\partial t}+(\boldsymbol{u}\cdot\nabla)p\right]=\frac{1}{R\sigma}[k\nabla^2T+\nabla k\cdot\nabla T]+\frac{(\gamma-1)M_e^2}{R}\Phi \tag{12}$$

$$\gamma M_e^2p=\rho T \tag{13}$$

where $\Phi=\lambda(\nabla\cdot\boldsymbol{u})^2+\mu/2[\nabla\boldsymbol{u}+\nabla\boldsymbol{u}^{tr}]^2$ is the viscous dissipation function, λ is the second coefficient of viscosity, γ is the ratio of specific heats, and $\boldsymbol{u}=(u,v,w)$. In addition, the Reynolds number is defined as $R=(\rho_e u_e l)/\mu_e$ and the Prandtl number, which is taken as a constant, as $\sigma=(\mu_e c_{p_e})/k_e$. Other variables are analogous to those in the boundary-layer equations presented previously.

We employ body-fitted orthogonal curvilinear coordinates x,y,z, where x is the streamwise direction, z is the azimuthal direction, and y is normal to the surface (see Fig. 1). In this system, elements of length are $h_1\,dx$, dy and $h_2\,dz$. In addition, we limit our study to two-dimensional or axisymmetric flows and make the quasiparallel flow assumption that restricts the mean flow to be of the following form: $\bar{u}=\bar{U}(y)$, $\bar{v}=0$, $\bar{w}=0$, $\bar{T}=\bar{T}(y)$, and $\bar{\rho}=\bar{\rho}(y)$. There is no a priori justification for the parallel flow approximation except at high Reynolds numbers, where it is formally valid depending on the disturbance characteristics. At finite Reynolds numbers, the parallel flow approximation introduces an unknown amount of error in the solution. The nonparallel multiple-scale calculations of Gapanov[19] and El-Hady[20] for Mach 4.5 flat-plate flow

show these effects to be small. The foregoing equations are decomposed into a mean part and small-amplitude harmonic disturbance of the form

$$u(x,y,z,t) = \bar{u}(y) + \epsilon\hat{u}(y)e^{i(\alpha x+\beta z-\omega t)} \tag{14a}$$

Here, ϵ is a small parameter, ω the disturbance frequency, α the x direction wavenumber, and β the z direction wavenumber. For an axisymmetric body of radius r_0,

$$\beta = n/r_0 \tag{14b}$$

where n is the wavenumber for asymmetric disturbances. We are interested in the spatial stability, so that ω and β are assumed real and α is complex.

Substituting the decompositions into the Navier-Stokes equations and dropping bars from the mean flow quantities, we obtain the following system of equations for the perturbation quantities (see Malik and Spall[12]):

$$\begin{aligned}&\frac{d^2\hat{u}}{dy^2} + (c_1T' + m_{23})\frac{d\hat{u}}{dy} + i\alpha l_1\frac{d\hat{v}}{dy} + c_1U'\frac{d\hat{T}}{dy}\\ &+ \left[ic_3R/\mu T - l_2\alpha^2 - \beta_0^2 + i\alpha l_2 m_{21} - l_2 m_{21}^2\right]\hat{u}\\ &+ \left[i\alpha(c_1T' + l_1m_{23}) - RU'/\mu T - m_{21}^2 l_2\right]\hat{v}\\ &- (i\alpha R/\mu)\hat{p} + \left[c_1\{U'' + m_{23}U' + i\alpha l_0 U m_{21} - l_2 U m_{21}^2\}\right.\\ &\left.+ c_2U'T'\right]\hat{T} - \left[\alpha\beta_0 l_1 + i\beta_0 l_3 m_{21}\right]\hat{w} = 0\end{aligned} \tag{15}$$

$$\begin{aligned}&\frac{d^2\hat{v}}{dy^2} + \frac{(i\alpha + m_{21})l_1}{l_2}\frac{d\hat{u}}{dy} + (c_1T' + m_{23})\frac{d\hat{v}}{dy}\\ &- \frac{R}{l_2\mu}\frac{d\hat{p}}{dy} + \frac{c_1Um_{21}l_0}{l_2}\frac{d\hat{T}}{dy} + \frac{i\beta_0 l_1}{l_2}\frac{d\hat{w}}{dy}\\ &+ \left[c_1T'(i\alpha + m_{21})l_0/l_2 - m_{21}m_{23}\right]\hat{u}\\ &+ \left[\frac{ic_3R/\mu T - \alpha^2 - \beta_0^2 + i\alpha m_{21} + c_1T'm_{23}l_0}{l_2} - m_{23}^2\right]\hat{v}\\ &+ \left[\frac{\{i\alpha c_1u' + c_1(U'm_{21}l_1 - Um_{21}m_{23}) + c_2UT'm_{21}l_0\}}{l_2}\right.\\ &\left.- c_1Um_{21}m_{23}\right]\hat{T}\\ &+ \left[i\beta_0(c_1T'l_0 - m_{23}l_3)/l_2\right]\hat{w} = 0\end{aligned} \tag{16}$$

$$\begin{aligned}&\frac{d\hat{v}}{dy} + (i\alpha + m_{21})\hat{u} + \left[m_{23} - T'/T\right]\hat{v} + \gamma M_e^2(m_{21}U - ic_3)\hat{p}\\ &- \left[(m_{21}U - ic_3)/T\right]\hat{T} + i\beta_0\hat{w} = 0\end{aligned} \tag{17}$$

$$\begin{aligned}&\frac{d^2\hat{T}}{dy^2} + c_4U'\frac{d\hat{u}}{dy} + (c_4Um_{21}l_0)\frac{d\hat{v}}{dy} + \left[\frac{2k'}{k} + m_{23}\right]\frac{d\hat{T}}{dy}\\ &+ c_4\left[i\alpha Um_{21}l_0 + Um_{21}^2l_2\right]\hat{u}\\ &+ \left[c_4(i\alpha U' + Um_{21}m_{23}l_2) - \sigma RT'/(\mu T)\right]\hat{v}\\ &- \left[ic_3c_4R/(2\mu)\right]\hat{p}\\ &+ \left\{ic_3R\sigma/(\mu T) - \alpha^2 - \beta_0^2 + i\alpha m_{21}\right.\\ &+ c_1c_4\left[(U'^2 + U^2m_{21}^2l_2)/2\right] + m_{23}k'/k + k''/k\Big\}\hat{T}\\ &+ (i\beta_0c_4Um_{21}l_2)\hat{w} = 0\end{aligned} \tag{18}$$

$$\begin{aligned}&\frac{d^2\hat{w}}{dy^2} + i\beta_0l_1\frac{d\hat{v}}{dy} + (c_1T' + m_{23})\frac{d\hat{w}}{dy} + (i\beta_0m_{21}l_3 - \alpha\beta_0l_1)\hat{u}\\ &+ i\beta_0(c_1T' + l_3m_{23})\hat{v} - (i\beta_0R/\mu)\hat{p} + (i\beta_0c_1Um_{21}l_2)\hat{T}\\ &+ \left[(ic_3 - m_{21}U)R/(\mu T) - \alpha^2 - l_2\beta_0^2 + i\alpha m_{21} - m_{21}^2\right.\\ &\left.- (c_1T' + m_{23})\right]\hat{w} = 0\end{aligned} \tag{19}$$

In the aforementioned equations,

$$(\,)' \equiv \frac{d}{dy}, \quad l_q = q + \frac{\lambda}{\mu}, \quad c_1 = \frac{1}{\mu}\frac{d\mu}{dT}, \quad c_2 = \frac{1}{\mu}\frac{d^2\mu}{dT^2}$$

$$c_3 = -(\alpha U - \omega), \quad c_4 = 2(\gamma - 1)M_e^2\sigma$$

The curvature coefficients m_{21} and m_{23} are defined as

$$m_{21} = \frac{1}{h_1h_2}\frac{\partial h_2}{\partial x}, \quad m_{23} = \frac{1}{h_2}\frac{\partial h_2}{\partial y}, \quad \beta_0 = \frac{\beta}{h_2}$$

In this study, we consider only cylinder and sharp cone configurations. For a cylinder $m_{21} = 0$ and $m_{23} = \epsilon/(1 + \epsilon y)$, where $\epsilon = l/r_0$. For a sharp cone, $m_{21} = [(l/r_0)\sin\lambda]/(1 + \epsilon y)$ and $m_{23} = \epsilon/(1 + \epsilon y)$, where λ is the cone half-angle and $\epsilon = (l\cos\lambda)/r_0$.

The foregoing equations are solved subject to the following boundary conditions:

$$\hat{u} = \hat{w} = \hat{v} = \hat{T} = 0 \quad \text{at} \quad y = 0 \tag{20a}$$

$$\hat{u}, \hat{v}, \hat{w}, \hat{T} \to 0 \quad \text{as} \quad y \to \infty \tag{20b}$$

The numerical scheme used to solve the stability equations is discussed in detail by Malik.[19] A brief description follows. Equations (15-19) are written in the form

$$(AD^2 + BD + C)\Phi = 0 \tag{21}$$

where Φ is a five-element vector defined as $(\hat{u},\hat{v},\hat{p},\hat{T},\hat{w})^{tr}$. The boundary conditions for Eq. (21) are given as

$$y = 0; \quad \Phi_1 = \Phi_2 = \Phi_4 = \Phi_5 = 0 \tag{22a}$$

$$y \to \infty; \quad \Phi_1, \Phi_2, \Phi_4, \Phi_5 \to 0 \tag{22b}$$

The transport coefficients have been expressed in terms of mean temperature and temperature perturbations as

$$\hat{\mu} = \frac{d\mu}{d\bar{T}}\hat{T}, \quad \hat{\lambda} = \frac{d\lambda}{d\bar{T}}\hat{T}, \quad \hat{k} = \frac{dk}{d\bar{T}}\hat{T}$$

Following Mack,[5] for temperatures greater than 198.6°R, Sutherland's law is used, whereas a linear relation is used for lower temperatures. A is a diagonal matrix defined as $[1,1,0,1,1]^{tr}$ and B and C are 5×5 coefficient matrices. The nonzero elements of these matrices depend on the mean flow quantities, streamwise and spanwise wavenumbers, and the disturbance frequency.

Both global and local methods are employed in the stability code. The global method, used to provide an initial guess for the local method, solves the stability equation in the form previously given. For the spatial problem, the streamwise wavenumber appears nonlinearly in Eq. (21). This nonlinearity arises from the streamwise diffusion terms. To use methods available for generalized eigenvalue problems, we linearize the equations by dropping the $\hat{u}_{xx}$ (i.e., α^2) terms. Since we are interested in hypersonic boundary layers in which the instability is generally inviscid in nature, and the global method is only used to provide a guess for the local method, the approximation is acceptable. The equations are discretized using a second-order finite-difference method on a staggered mesh. The staggered mesh eliminates the need for pressure boundary con-

ditions. The discretized equations are expressed in the form of a generalized eigenvalue problem as

$$\bar{A}\Phi = \alpha \bar{B}\Phi \tag{23}$$

which may be solved using the QZ algorithm.

The global solution is computationally expensive since the results include all the eigenvalues of the discrete system. As a result, a local method is used to refine the accuracy of the desired least stable eigenvalue. The local method is based on the fourth-order compact finite-difference scheme of Malik et al.[21] The scheme requires that Eq. (21) be written as a system of first-order equations as

$$\frac{d\Psi_i}{dy} = \sum_{j=1}^{8} a_{ij}\Psi_j; \qquad i = 1,2,\ldots,8 \tag{24}$$

where

$$\Psi_1 = \Phi_1, \quad \Psi_2 = \frac{d\Phi_1}{dy}, \quad \Psi_3 = \Phi_2, \quad \Psi_4 = \Phi_3$$

$$\Psi_5 = \Phi_4, \quad \Psi_6 = \frac{d\Phi_4}{dy}, \quad \Psi_7 = \Phi_5, \quad \Psi_8 = \frac{d\Phi_5}{dy}$$

with boundary conditions

$$y = 0; \qquad \Psi_1 = \Psi_3 = \Psi_5 = \Psi_7 = 0 \tag{25a}$$

$$y \to \infty; \qquad \Psi_1, \Psi_3, \Psi_5, \Psi_7 \to 0 \tag{25b}$$

The fourth-order-accurate compact finite-difference scheme is derived by means of the Euler-Mclaurin sum formula

$$Y^k - Y^{k-1} = \frac{h_k}{2}\left(\frac{dY^k}{dy} + \frac{dY^{k-1}}{dy}\right) - \frac{h_k^2}{12}\left(\frac{dY^k}{dy^2} - \frac{d^2Y^{k-1}}{dy^2}\right) + \mathcal{O}(h_k^5) \tag{26}$$

where $Y^k = Y(y_k)$ and $h_k = y_k - y_{k-1}$. Expressions for the derivatives of Y in Eq. (26) are replaced using Eq. (24), where we define $Y = \{\Psi_i\}$. This results in a system that can be written as

$$\Psi_i^k - \frac{h_k}{2}\sum_{j=1}^{8} a_{ij}^k\Psi_j^k + \frac{h_k^2}{12}\sum_{j=1}^{8} b_{ij}^k\Psi_j^k - \left[\Psi_i^{k-1} + \frac{h_k}{2}\sum_{j=1}^{8} a_{ij}^{k-1}\Psi_j^{k-1} + \frac{h_k^2}{12}\sum_{j=1}^{8} b_{ij}^{k-1}\Psi_j^{k-1}\right] = 0 \qquad i = 1,2,\ldots,8 \tag{27}$$

where

$$b_{ij} = \frac{da_{ij}}{dy} + \sum_{m=1}^{8} a_{im}a_{mj}$$

Equation (27) is rewritten in block tridiagonal form as

$$A_kY^{k-1} + B_kY^k + C_kY^{k+1} = H \tag{28}$$

where A_k, B_k, C_k are 8×8 matrices and H is an 8×1 null matrix. The block tridiagonal system of equations is solved using LU factorizations. Since Eq. (27) and the boundary conditions are homogeneous, a trivial solution may result. In order to avoid this, the boundary condition $\Psi_1(0) = 0$ is replaced with the nonhomogeneous pressure boundary condition $\Psi_4(0) = 1$. With an initial guess for α, a nontrivial solution to Eq. (28) can now be obtained for Y. Newton's method is then used to iterate on α until the boundary condition $\Psi_1 = 0$ is satisfied. The foregoing procedure is described in detail by Malik.[22]

Results and Discussion

In this section, we discuss the results of the stability calculations for a series of sharp cones and hollow cylinders at a boundary-layer edge Mach number of 5.0. The majority of results are presented in the form of N-factor calculations that can be performed in several ways. The N-factor is computed as

$$N(f) = -\int_{x_0}^{x} \alpha_i(x)\,dx \tag{29}$$

where x_0 is the streamwise location of the onset of instability for the dimensional frequency f. A choice must be made regarding the prescription of the wavenumber β. For the purpose of this paper, β has been chosen to maximize the disturbance growth rate. For first mode disturbances, this is done by enforcing the condition $d\alpha_i/d\beta = 0$ at each streamwise location, which amounts to constructing an envelope for the individual growth rate curves for fixed n [see Eq. (14b)]. For second mode disturbances, the foregoing condition is satisfied for $\beta = 0$ (i.e., $n = 0$), since in that case, two-dimensional (or axisymmetric) waves are most amplified. The effect of transverse curvature on the most unstable wave angles for first mode disturbances is discussed in the work of Malik and Spall.[12]

We first examine the effects of transverse curvature on the linear stability of a series of boundary layers formed over hollow cylinders. The freestream Mach number is 5.0, the stagnation temperature 540°R, and the unit Reynolds number 1 million. Adiabatic wall conditions are specified for all mean flows. Note that in the figures to follow, the Reynolds number is plotted as $R = u_e l/v_e$, where the length scale l is defined as $l = \sqrt{v_e x/u_e}$. Thus, $R = \sqrt{Re_x}$, where Re_x is the usual Reynolds number based on the streamwise distance x. We also define a "cylinder" Reynolds number as $R_0 = u_e r_0/v_e$, which is simply the unit Reynolds number times the cylinder radius. The nondimensional frequency F is given as $F = (2\pi v_e)/(U_e^2)f$. For the N-factor calculations, the most dangerous frequencies (those that first reach $N = 9$) have been determined to within $\pm 10\%$. We note that for all the cylinder configurations, curvature terms have been included in both the mean flow and stability calculations. We will later note that, for a given Mach number flow, the effect of curvature scales with the cylinder Reynolds number R_0.

Neutral stability curves are presented in Fig. 2a for the flat-plate case and in Fig. 2b for the case $r_0 = 0.025$ ft, or $R_0 = 2.5\times 10^4$. These represent the limiting cases for no curvature and large curvature, respectively, in the N-factor calculations for cylinders that follow. The most prominent difference in the neutral curves is the separation of the first and second mode unstable regions, which is attributable to curvature effects (Fig. 2b). This separation is due to the second mode region where the instabilities have been shifted to higher frequencies. In addition, we see a significant narrowing of the unstable frequency band. The upward shift is not unexpected since increasing transverse curvature in the mean flow results in a thinning of the boundary layer due to transverse curvature effects. Since second mode instabilities scale with the boundary-layer thickness, the unstable band occurs at higher frequencies. It also appears that at high Reynolds numbers, the second mode instability may be completely damped. This is because as the boundary-layer thickness increases, transverse curvature effect will increase for a fixed cylinder radius. We note that transverse curvature effects on the first mode region are not significant, although the maximum unstable frequencies at low Reynolds numbers are increased by some 20%. A detailed discussion of these effects is presented by Malik and Spall.[12] They indicate increased growth rates for the oblique first mode waves and decreased growth rates for the second mode, as curvature is increased, which is consistent with the results in Figs. 2a and 2b. The question is what effect this will have on the integrated amplification rates.

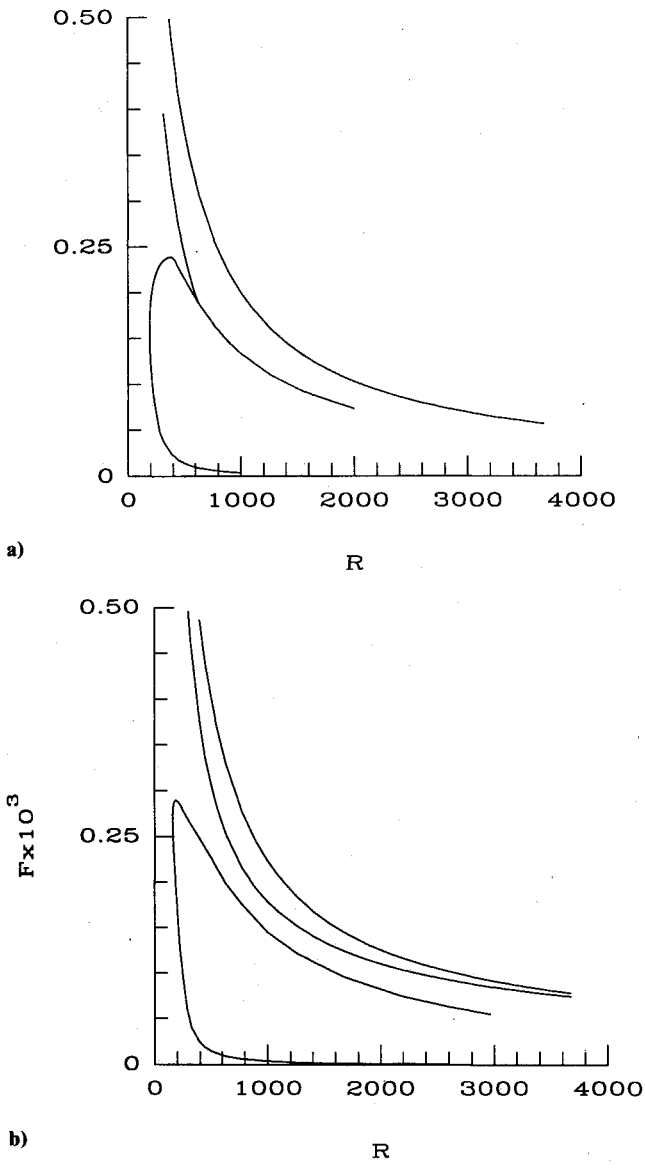

Fig. 2 Neutral stability curves for Mach 5 boundary layer: a) Flat plate; b) $r_0 = 0.025$ ft.

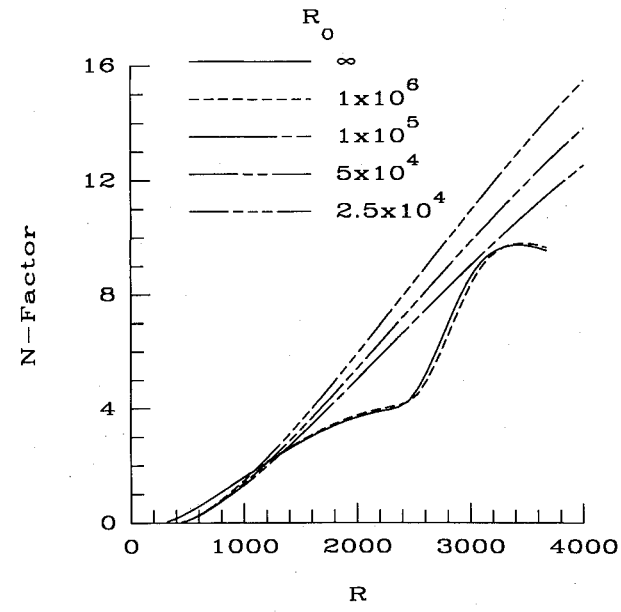

Fig. 3 N-factor calculations for flat plate and cylinders.

We next examine N-factor calculations for a series of cylinders. These calculations are shown in Fig. 3 for increasing levels of transverse curvature, i.e., $R_0 = \infty$, 1×10^6, 1×10^5, 5×10^4, and 2.5×10^4 ($r_0 = \infty$, 1.0, 0.1, 0.05, and 0.025 ft). The lines in the figure do not represent the envelope curves, but the frequencies that first reach $N = 9$. The illustration also indicates that as the Reynolds number R_0 is increased from 2.5×10^4 to ∞, R_{tr} is increased from 2600 to 3050. For the cases $R_0 = 2.5 \times 10^4$, 5×10^4, and 1×10^5, the second mode has no effect on transition location and the increase in N is due to first mode instabilities only. For the flat-plate case and the case of $R_0 = 1 \times 10^6$, second mode instabilities influence transition location due to their large amplification rates at higher Reynolds numbers. Thus, we conclude that first mode disturbances are destabilized with increasing curvature.

The results of Malik and Spall[12] lead one to expect the foregoing results. For instance, they showed that the effect of increasing curvature is to stabilize and shift the second mode instability to higher frequencies—thus, the absence of any second mode effect on transition location for the cases with the relatively small radius of curvature. What the second mode instabilities do cause, though, is an abrupt increase in the frequency responsible for transition, as curvature is decreased. For instance, in the case of the flat plate, the most amplified frequency is $F = 0.6 \times 10^{-4}$, corresponding to a second mode disturbance. For cylinder radii from 0.025 to 0.1 ft, the most amplified frequency is $F = 0.27 \times 10^{-4}$, which corresponds to a first mode disturbance. This is due to the effect that transverse curvature has on first mode (destabilizing) and second mode (stabilizing) instabilities. In other words, as curvature increases, low-frequency first mode instabilities begin to influence the N-factor calculations and transition location. These trends are, of course, only valid in the ranges of frequencies that, under the present conditions, are important for transition.

We now look at a series of calculations for 2, 5, and 10-deg half-angle cones at a zero angle of attack. The flow conditions at the boundary-layer edge are identical to those of the cylinder calculations. Calculations are made both with and without curvature terms in the mean flow equations. Curvature terms are included in the stability equations for all calculations. For the sharp cone, the m_{21} term in the stability equations is nonzero. This term is due to the body divergence and is proportional to dr_0/dx. Thus, we expect m_{21} to be important for large cone angles, and m_{23} to be important for small angles. This, in fact, was shown by Malik and Spall.[12] We also note that although the effect of curvature on stability and mean flow increase in the streamwise direction for hollow cylinders, the opposite is true for the cone. This is a result of the greater rate of increase in r_0 compared to the boundary-layer thickness as the flow develops in the streamwise direction.

Presented in Fig. 4 are N-factor calculations for 2, 5, and 10-deg half-angle sharp cones in which the curvature terms are included in both the mean flow and stability calculations. Although not apparent from the figures, the integrated amplification rates are due to first mode instabilities. We first compare the ratio of cone to flat-plate transition Reynolds number for the different cone angles. Note that in the following discussion, transition is assumed to occur when $N = 9$. This ratio may vary slightly if, for instance, N is taken as 10. For the 2, 5, and 10-deg cones, the ratio $Re_{tr_{cone}}/Re_{tr_{plate}} \approx 0.80$, 0.85, and 0.85, respectively. This is consistent with the results of Malik and Spall,[12] in which they indicate that first mode instability is enhanced through increased curvature. These values are somewhat higher than the value of 0.68 reported by Chen et al.[4] for a 5 deg cone at $M_\infty = 3.5$. In that study, transition was assumed to occur when N reached 10. The frequencies responsible for transition over the cone configuration are in the vicinity of $F = 0.4 \times 10^{-4}$. This compares to the frequency of $F = 0.6 \times 10^{-4}$ for the flat-plate case discussed earlier. The flat-plate frequency is higher due to the effect of the second mode. If, for the flat plate, first mode disturbances only were

considered, the most amplified frequency would be approximately $F=0.27\times10^{-4}$. This second mode influence also increases the ratio $Re_{tr_{cone}}/Re_{tr_{plate}}$ and is partially responsible for the differences with the results of Chen et al.[4] where only first mode instabilities were encountered. We thus conclude that the ratio of cone to flat-plate transition Reynolds number is highly dependent on the flow conditions. This is especially true for high supersonic Mach numbers, where both first and second mode instabilities are significant.

We now examine the effect of neglecting the curvature terms in the mean flow equations. The N-factor calculations are presented in Fig. 5. In this case, the ratio of cone to flat-plate transition Reynolds number is approximately 0.7, 0.95, and 1.05 for 2, 5, and 10-deg cone angles, respectively. Thus, neglecting curvature terms results in a destabilizing effect for small cone angles and a stabilizing effect for larger angles. This indicates competing mechanisms affecting the first mode instability: The curvature terms in the mean flow equations are stabilizing while body divergence terms are destabilizing. This is the opposite effect that curvature and body divergence terms have in the stability equations.[12] We can conclude that a complex relation exists between the curvature terms in the mean flow and stability equations, and that their relative importance is highly dependent on the specific geometry and flow conditions.

As suggested by Morkovin,[21] nonsimilarity of the mean flow profile may, in principle, bring about some unit Reynolds number effect. The thin cylinder profiles we have been investigating are nonsimilar due to curvature effect. We now investigate the possibility that this nonsimilarity manifests itself in the form of an "apparent" unit Reynolds number effect. We compute N-factors for three unit Reynolds numbers—250,000/ft, 1 million/ft, and 4 million/ft—at a constant cylinder radius of 0.025 ft. The results shown in Fig. 6a for the three different values of the cylinder Reynolds number (R_0) are dramatic. The streamwise location of transition is delayed by a factor of 2 when R_0 is increased from 6.25×10^3 to 1×10^5 (at a constant cylinder radius). This unit Reynolds number effect, which one may observe in an experiment performed on a fixed radius cylinder, is actually a transverse curvature effect. At any rate, Fig. 6a shows that transverse curvature effects, which for the first mode are destabilizing, become more important as R_0 is decreased. We also note that the most amplified nondimensional frequency decreases in accordance with an increase in the cylinder Reynolds number.

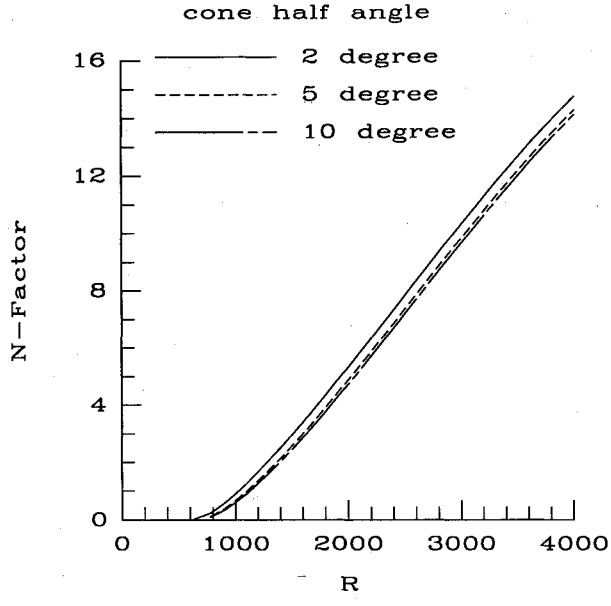

Fig. 4 N-factor calculations for cones in which curvature terms are included in mean flow and stability equations.

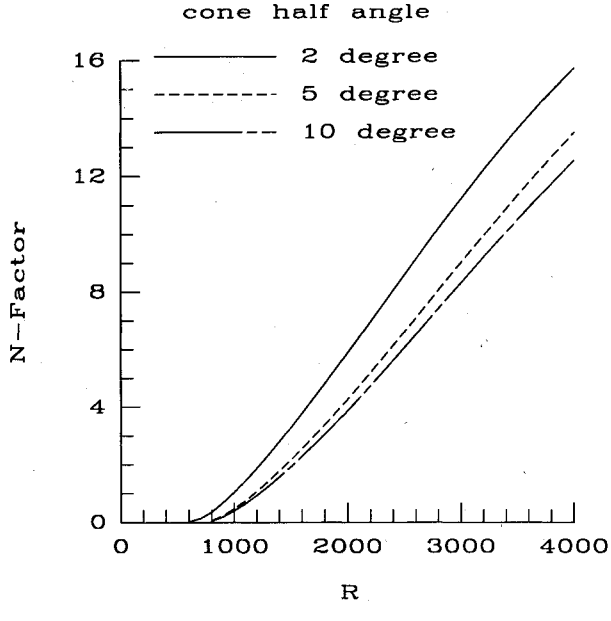

Fig. 5 N-factor calculations for cones. Curvature terms included in stability equations but neglected in the mean flow.

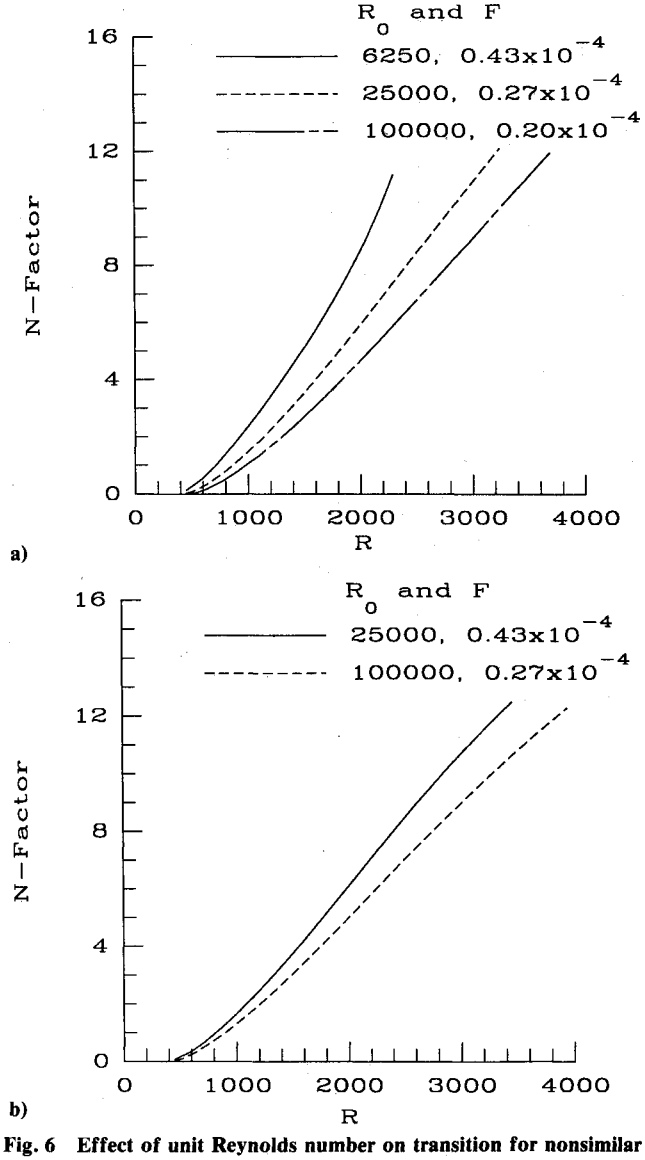

Fig. 6 Effect of unit Reynolds number on transition for nonsimilar boundary layers over hollow cylinders: a) $r_0=0.025$ ft; b) $r_0=0.1$ ft.

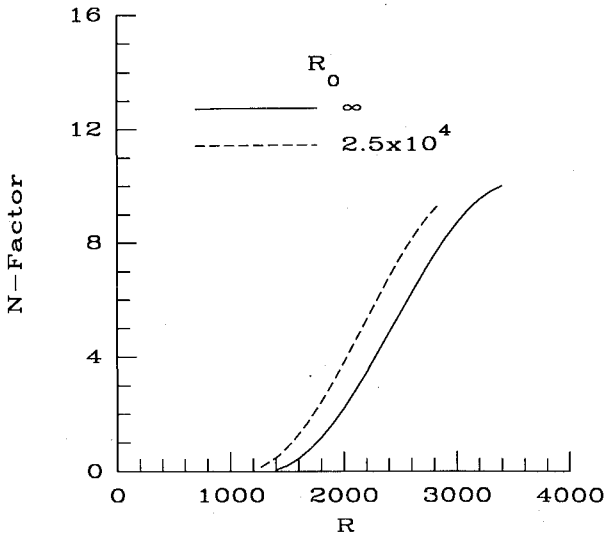

Fig. 7 *N*-factor calculations for cylinders at Mach 1.25.

We now look at N-factors for the case $r_0 = 0.1$ ft, shown in Fig. 6b. Here, results for unit Reynolds numbers of 2.5×10^5 ($R_0 = 2.5 \times 10^4$) and 1×10^6 ($R_0 = 1 \times 10^5$) are plotted. The results are similar to those in Fig. 6a in that as R_0 (or unit Reynolds number) is increased, transition is delayed. From Figs. 6a and 6b, it is clear that transition occurs at nearly constant Re_x for a given R_0. The cylinder Reynolds number R_0 characterizes the effect of transverse curvature. Therefore, the preceding results for $r_0 = 0.025$ ft, for examples, are applicable to a cylinder with larger radius as long as R_0 is held fixed.

To demonstrate that transverse curvature effects are important throughout the supersonic flow regime, we present results for a Mach 1.25 boundary layer over a cylinder. The mean flow stagnation temperature was 540°R and the unit Reynolds number, 1 million. N-factor results are shown in Fig. 7. Lines for a flat plate and a cylinder radius $r_0 = 0.025$ ft ($R_0 = 2.5 \times 10^4$) are indicated. Clearly, the influence of transverse curvature at Mach 1.25 is comparable to that at Mach 5.0.

At lower Mach numbers, the boundary layer is thinner and thus the curvature parameter $\delta_{0.995}/r_0$ is smaller for the same cylinder radius r_0. However, the sensitivity of the lower Mach number boundary layer to any changes in curvature, heat transfer, etc., is greater than at higher Mach numbers. Thus, the decrease in curvature parameter is compensated for by the enhanced sensitivity of the boundary layer at lower Mach numbers.

Conclusions

N-factor calculations for Mach 5 flow past a series of cylinder and cone configurations were performed. The purpose of the calculations was to assess the importance, in regard to transition prediction, of transverse curvature terms in the mean flow and stability equations. The results indicate that for thin cylinders and small cone angles, the terms should not be neglected. At Mach 5, transition on a flat plate was found to be dependent on both first and second mode instabilities. Conversely, for a cone, transition was dependent on first mode only. The net result was to increase the ratio of $Re_{tr_{cone}}/Re_{tr_{plate}}$ over that found by Chen et al.[4] It was also found that transverse curvature introduced a unit Reynolds number effect on the location of transition. As the unit Reynolds number was increased, the onset of transition, based on the e^N method, was delayed. This is in accordance with experimental findings. Transverse curvature effects were also shown to be destabilizing at a Mach number of 1.25. We also note that the effect of transverse curvature may be characterized by the Reynolds number based on the cylinder radius.

Acknowledgment

The authors would like to thank Ajay Kumar, Theoretical Flow Physics Branch, NASA Langley Research Center, for support of this work under NAS1-18240.

References

[1]Pate, S. R., "Measurements and Correlations of Transition Reynolds Numbers on Sharp Slender Cones at High Speeds," *AIAA Journal,* Vol. 9, No. 6, 1971, pp. 1082–1090.

[2]Mack, L. M., "Stability of Axisymmetric Boundary Layers on Sharp Cones at Hypersonic Mach Numbers," AIAA Paper 87-1413, June 1987.

[3]Malik, M. R., "Prediction and Control of Transition in Hypersonic Boundary Layers," AIAA Paper 87-1414, June 1987.

[4]Chen, F.-J., Malik, M. R., and Beckwith, I. E., "Boundary-Layer Transition on a Cone and Flat Plate at Mach 3.5," *AIAA Journal,* Vol. 27, No. 6, 1989, pp. 687–693.

[5]Mack, L. M., "Boundary Layer Linear Stability Theory," AGARD-R-709, June 1984.

[6]Lees, L., "The Stability of the Laminar Boundary Layer in a Compressible Fluid," NACA TR 876, 1947.

[7]Mack, L. M., "Boundary Layer Stability Theory," Jet Propulsion Lab., Pasadena, CA, Doct. 900-277, Rev. A, 1969.

[8]Demetriades, A., "New Experiments on Hypersonic Boundary Layer Stability Including Wall Temperature Effects," *Proceedings of the Heat Transfer and Fluid Mechanics Institute,* Pullman, Washington, 1978, pp. 39–55.

[9]Malik, M. R., "Instability and Transition in Supersonic Boundary Layers. Laminar-Turbulent Boundary Layers," *Proceedings of Energy Resources Technology Conference,* edited by E. M. Uram and H. E. Weber, American Society of Mechanical Engineers, New York, Feb. 1984, pp. 139–147.

[10]Gasperas, G., "The Stability of the Compressible Boundary Layer on a Sharp Cone at Zero Angle of Attack," AIAA Paper 87-0494, Jan. 1987.

[11]Gasperas, G., "Effect of Wall Temperature Distribution on the Stability of the Compressible Boundary Layer," AIAA Paper 89-1894, June 1989.

[12]Malik, M. R., and Spall, R. E., "On the Stability of Compressible Flow Past Axisymmetric Bodies," High Technology Rept. HTC-8905, 1989.

[13]Duck, P. W., "The Inviscid Axisymmetric Stability of the Supersonic Flow Along a Circular Cylinder," NASA CR-181816, 1989.

[14]Kendall, J. M., "Wind Tunnel Experiments Relating to Supersonic and Hypersonic Boundary-Layer Transition," *AIAA Journal,* Vol. 13, No. 3, 1975, pp. 290–299.

[15]Demetriades, A., "Laminar Boundary Layer Stability Measurements at Mach 7 Including Wall Temperature Effects," AFOSR TR-77-1311, 1977.

[16]Stetson, K. F., Thompson, E. R., Donaldson, J. C., and Siler, L. G., "Laminar Boundary Layer Stability Experiments on a Sharp Cone at Mach 8, Part 1: Sharp Cone," AIAA Paper 83-1761, July 1983.

[17]Harris, J. E., and Blanchard, D. K., "Computer Program for Solving Laminar, Transitional, or Turbulent Compressible Boundary-Layer Equations for Two-Dimensional and Axisymmetric Flow," NASA TM-83207, Feb. 1982.

[18]Probstein, R. F., and Elliot, D., "The Transverse Curvature Effects in Compressible Axially Summetric Boundary-Layer Flow," *Journal of Aeronautical Science,* Vol. 23, March 1956, pp. 208–224.

[19]Gapanov, S. A., "The Influence of Flow Non-parallelism on Disturbance Development in the Supersonic Boundary Layer," *Proceedings of the 8th Canadian Congress of Applied Mechanics,* Montreal, 1983, pp. 673, 674.

[20]El-Hady, N. M., "On the Effect of Boundary Layer Growth on the Stability of Compressible Flows," NASA CR-3474, 1981.

[21]Malik, M. R., Chuang, S., and Hussaini, M. Y., "Accurate Numerical Solution of Compressible, Linear Stability Equations," *ZAMP,* Vol. 33, March 1982, pp. 189–201.

[22]Malik, M. R., "Numerical Methods for Hypersonic Boundary Layer Stability," *Journal of Computational Physics,* Vol. 86, Feb. 1990, pp. 376–413.

[23]Morkovin, M. V., "Critical Evaluation of Transition from Laminar to Turbulent Shear Layers with Emphasis on Hypersonically Traveling Bodies," AFFDL-TR-68-149, Air Force Flight Dynamics Lab., Wright-Patterson AFB, OH, March 1969.